doi:10.1093/brain/awq209 Brain 2010: 133; 2714–2726 | 2714

BRAIN
A JOURNAL OF NEUROLOGY

Disruption of odour quality coding in piriform cortex mediates olfactory deficits in Alzheimer's disease

Wen Li,[1,2] James D. Howard[3] and Jay A. Gottfried[3,4]

1 Department of Psychology, University of Wisconsin–Madison, Madison, WI 53706, USA
2 The Waisman Centre, University of Wisconsin–Madison, Madison, WI 53706, USA
3 Department of Neurology, Northwestern University Feinberg School of Medicine, Chicago, IL 60611, USA
4 The Cognitive Neurology and Alzheimer's Disease Centre, Northwestern University Feinberg School of Medicine, Chicago, IL 60611, USA

Correspondence to: Dr Wen Li,
Department of Psychology,
University of Wisconsin-Madison,
1202 W. Johnson Street, Madison,
WI 53706, USA
E-mail: wenli@psych.wisc.edu

Patients with early-stage Alzheimer's disease exhibit perceptual deficits in odour identification, often before the appearance of overt memory loss. This impairment coincides with the initial accumulation of pathological lesions in limbic olfactory brain regions. Although these data imply that odour stimuli may be effectively used as biological probes of limbic dysfunction, the precise neural mechanisms underlying the olfactory deficits in early Alzheimer's disease remain poorly understood. In the current study, we combined functional magnetic resonance imaging with an olfactory cross-adaptation paradigm to test the hypothesis that perceptual codes of odour quality in posterior piriform cortex are degraded in patients with Alzheimer's disease. In elderly control subjects, sequential presentation of qualitatively similar (versus qualitatively different) odourant pairs elicited cross-adapting responses in posterior piriform cortex, in accord with the pattern observed in healthy young adults. However, this profile was significantly blunted in patients with Alzheimer's disease, reflecting a functional disruption of odour quality coding in this olfactory brain area. These results highlight the potential of olfactory functional magnetic resonance imaging as a non-invasive bioassay of limbic functional integrity, and suggest that such an index could possibly aid in the early diagnosis of Alzheimer's disease. Furthermore, as a putative lesion model of odour quality processing in the human brain, our study suggests a causal role of posterior piriform cortex in differentiating olfactory objects.

Keywords: Alzheimer's disease; olfactory identification deficit; odour quality coding; functional magnetic resonance imaging cross-adaptation; piriform cortex

Abbreviations: fMRI = functional magnetic resonance imaging; MMSE = Mini-Mental State Examination; PPC = posterior piriform cortex

Introduction

Alzheimer's disease is a neurodegenerative disorder typified by progressive memory loss and cognitive debilitation that currently afflicts as many as 5 million people in the USA alone (Hebert *et al.*, 2003). Its pathological hallmark is the accumulation of neurofibrillary tangles and amyloid plaques throughout limbic and paralimbic regions of the brain (Braak and Braak, 1991;

Received January 7, 2010. Revised June 14, 2010. Accepted June 18, 2010

Mesulam, 2000). With disease progression, the distribution of tangles and plaques expands beyond the limbic system into heteromodal cortical areas, leading to global deficits spanning memory, attention, language, visuospatial skills and comportment. By contrast, the primary sensory (i.e. visual, auditory and somatosensory) cortices are minimally affected (Pearson *et al.*, 1985), such that basic sensory perception tends to be spared, even in end-stage cases.

The one exception to this rule is the sense of smell: olfactory perception is commonly disrupted in Alzheimer's disease. Indeed, smelling impairments often coincide with, or precede, the onset of classical cognitive problems such as overt memory loss (Doty *et al.*, 1987; Koss *et al.*, 1988; Morgan *et al.*, 1995; Moberg *et al.*, 1997; Mesholam *et al.*, 1998; Royet *et al.*, 2001; Djordjevic *et al.*, 2008). Despite some initial conflicts in the literature, it is now evident that patients with early-stage Alzheimer's disease have both lower-level deficits of odour detection (e.g. threshold sensitivity) and higher-order deficits of odour quality perception (e.g. discrimination and identification). A 1998 meta-analytic review documented substantial impairment across all domains of olfactory perception, including detection, identification and memory (Mesholam *et al.*, 1998). Recent longitudinal studies indicate that behavioural performance on a smell identification/discrimination test can help identify patients at risk for Alzheimer's disease (Devanand *et al.*, 2000, 2008; Schubert *et al.*, 2008), highlighting the potential impact that olfactory-based measures and biomarkers may hold for pre-clinical diagnosis. Interestingly, this dysfunction appears to be specific to odourous stimuli, as gustatory and visual discriminations remain intact (Koss *et al*., 1988; Murphy *et al*., 1990).

It is likely that olfactory impairment in early Alzheimer's disease reflects the anatomical intersection of early Alzheimer's pathology with limbic brain regions involved in olfactory processing, including the anterior olfactory nucleus, piriform cortex, amygdala and entorhinal cortex (Herzog and Kemper, 1980; Averback, 1983; Hyman *et al.*, 1984; Pearson *et al.*, 1985; Reyes *et al.*, 1987). Distinctive histopathological lesions are also seen in olfactory sensory neurons (Talamo *et al.*, 1989) and the olfactory bulb (Ohm and Braak, 1987), as well as in higher-order olfactory projections terminating in the orbitofrontal cortex, insula and hippocampus (Mesulam, 2000). Neuroimaging work further reveals morphological changes (Kesslak *et al.*, 1991; Murphy *et al.*, 2003; Thomann *et al.*, 2009) and functional anomalies (Buchsbaum *et al.*, 1991; Kareken *et al.*, 2001; Murphy *et al.*, 2005) in olfactory structures. Nevertheless, the precise neurobiological correlates of the smell identification deficits in Alzheimer's disease remain unknown.

Recent work in rodents (Kadohisa and Wilson, 2006) and humans (Gottfried *et al.*, 2006; Li *et al.*, 2006, 2008; Howard *et al.*, 2009) indicates that the posterior piriform cortex (PPC), a three-layer paleocortex situated within the medial temporal lobe, plays an important role in odour quality coding. Human functional magnetic resonance imaging (fMRI) studies indicate that this limbic brain region preferentially encodes the perceptual quality, or character, of a smell emanating from an odourous object (Gottfried *et al.*, 2006) and is a target of learning-induced plasticity in quality-based representations (Li *et al.*, 2006, 2008). Recently we have shown that ensemble fMRI activity patterns in human PPC align with categorical percepts of odour qualities (Howard *et al.*, 2009). Given that information about odour quality is encoded in PPC, and given that PPC itself is an early target of Alzheimer's disease neuropathology, it follows that degraded perceptual representations of odour quality in PPC may underlie the behavioural deficits of odour discrimination and identification in patients with mild Alzheimer's disease.

To examine the integrity of PPC odour quality coding in early-stage patients with Alzheimer's disease, we implemented an olfactory version of fMRI cross-adaptation. This imaging technique is based on the rationale that sequential presentation of stimuli sharing a particular feature (e.g. object size, facial identity) induces adaptation of neural populations specifically sensitive to that feature, leading to local response suppression (Buckner *et al.*, 1998; Kourtzi and Kanwisher, 2001; Grill-Spector *et al.*, 2006). In our previous work (Gottfried *et al.*, 2006), young healthy subjects (mean age 25 years) participated in an olfactory fMRI adaptation paradigm as they made two sniffs in succession and smelled pairs of odourants that systematically varied in perceptual quality. Odour-evoked fMRI activity in PPC significantly decreased (cross-adapted) in response to qualitatively similar, but not to qualitatively dissimilar, odourant pairs, supporting the idea of odour quality coding in this brain region.

Therefore, in the present study, we utilized an olfactory fMRI cross-adaptation paradigm to test whether posterior piriform representations of odour quality are disorganized in patients with mild Alzheimer's disease. The central hypothesis was that the olfactory discrimination impairment in early Alzheimer's disease reflects a specific disruption of odour quality coding, typified by widening and overlap of neural tuning curves in PPC (Fig. 1). As a consequence, we predicted that comparable magnitudes of fMRI adaptation would be observed following presentation of similar quality and different quality odourant pairs, in effect, highlighting a loss of response specificity for odour quality. Concurrent examination of other limbic olfactory areas also known to be affected in Alzheimer's disease enabled us to determine whether the breakdown of odour quality coding was regionally specific for PPC. Finally, by analysing olfactory fMRI adaptation at the level of individual voxels across piriform cortex, we were able to gain a more mechanistic understanding of how odour quality coding in PPC is disrupted in mild-stage Alzheimer's disease, in comparison with age-matched control subjects.

Materials and methods

Subjects

Ten patients with Alzheimer's disease (six females) and 10 normal controls, matched for age and sex, were recruited from the Clinical Core subject registry of the Northwestern University Alzheimer's Disease Centre, except for one control subject who was recruited from the community. All subjects provided informed consent to take part in the study, which was approved by the Northwestern University Institutional Review Board. Prior to enrolment in the study, subjects

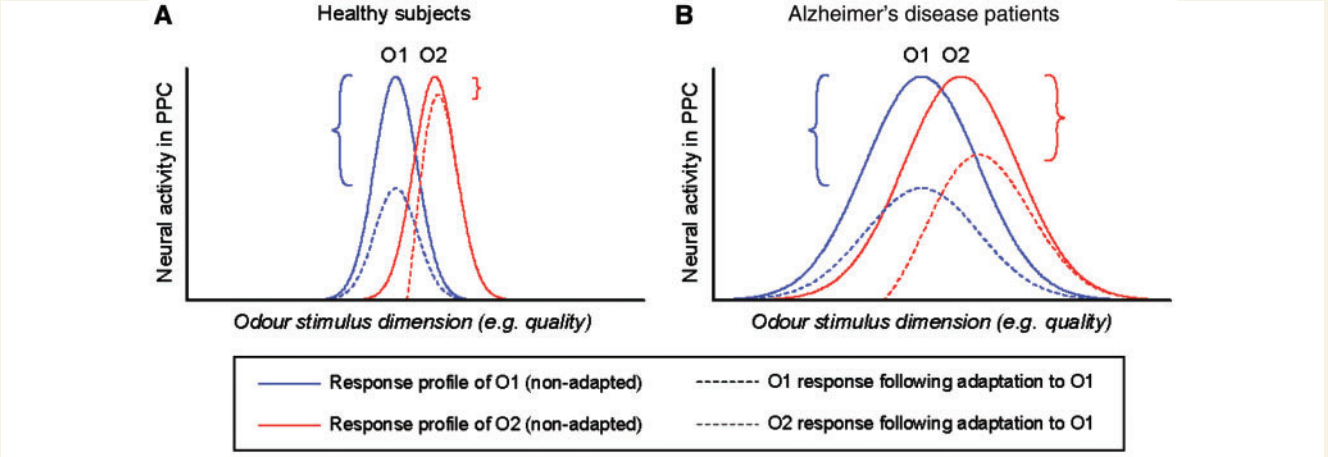

Figure 1 Schematic model illustrating the disruption of odour quality coding in Alzheimer's disease and its impact on olfactory cross-adaptation. (**A**) In healthy subjects, the tuning curves in PPC demonstrate a modest degree of population overlap for two qualitatively distinct odourants (O1, solid blue line; O2, solid red line). Initial presentation of O1 induces adaptation of O1-responsive neurons (dashed blue line) and a reduction in neural activity (blue bracket). However, because some of the O1 neurons also respond to O2, the presentation of O1 will induce adaptation in a subset of O2-responsive neurons (red dashed line), resulting in a small reduction of neural activity when O1 is sequentially followed by O2 (red bracket). (**B**) In patients with Alzheimer's disease, the prediction is that a loss of coding specificity for odour quality will yield wider and more overlapping tuning curves for O1 and O2. As a consequence, initial presentation of O1 will elicit adaptation in a larger subset of O2-responsive neurons (red dashed line), with a correspondingly greater decline in neural activity when O1 is followed by O2 (red bracket), and similar in magnitude to that elicited by repeated presentations of O1 (blue bracket).

were screened to ensure that odour detection thresholds were matched across both groups.

At the time of their initial medical visit to the Alzheimer's Centre, each patient with Alzheimer's disease was informed of the Clinical Core and asked to participate for the purposes of research and/or clinical trials. Upon entry into the Clinical Core, patients and healthy subjects all provided detailed demographic and medical histories, and they all received comprehensive neurological and neuropsychological examinations. The diagnosis of mild probable Alzheimer's disease was made on the basis of diagnostic criteria of the National Institute of Neurological and Communicative Disorders and Stroke and the Alzheimer's Disease and Related Disorders Association for retentive memory impairment, the presence of deficits in one other cognitive domain sufficient to cause a disruption in customary activities of daily living (McKhann *et al.*, 1984) and a score of $\geq$20 on the Mini-Mental State Examination (MMSE; Folstein *et al.*, 1975). Control subjects were community-dwelling, cognitively intact healthy older adults, without any history of medical, neurological or psychiatric disorder, substance abuse, or tobacco use, who were originally recruited through advertisements or community outreach programs. None performed more than 2 SD below the age-appropriate mean scores on the neuropsychological test battery and none had difficulties with daily living activities.

Stimuli

We used the same four odourants as used in our previous study that investigated olfactory perceptual learning of odour quality and odourant structure (Gottfried *et al.*, 2006). These odourants included two 'minty' smells comprising one ketone (L-carvone; CV, 5%) and one alcohol (DL-menthol; MT, 10%), and two 'floral' smells also comprising one ketone (acetophenone, 0.1%) and one alcohol (phenethyl alcohol, 5%), all diluted in mineral oil and roughly matched for intensity. Odourants were delivered using an MRI-compatible, 10-channel computer-controlled olfactometer (airflow set at 3 l/min), which permits rapid delivery of odour in the absence of tactile, thermal or auditory confounds (Gottfried *et al.*, 2006; Li *et al.*, 2006). Stimulus presentation and collection of intensity ratings were controlled using Cogent2000 software (Wellcome Department, London, UK), as implemented in Matlab (Mathworks, Natick, MA).

Paradigm

Subjects took part in an olfactory fMRI cross-adaptation study that closely corresponded to a paradigm previously conducted in our laboratory, in healthy young individuals (Li *et al.*, 2006). In each trial, subjects made two consecutive sniffs and smelled a pair of odourants that were either similar or different in odour perceptual quality, and either similar or different in odourant molecular functional group. This constituted four trial types: same quality/same group (SQ/SG); same quality/different group (SQ/DG); different quality/same group (DQ/SG); and different quality/different group (DQ/DG). As a fifth control trial type, we also included trials in which odourless room air was presented at the second sniff (Fig. 2).

The fMRI experiment consisted of two runs of 40 trials, with 8 trials per each of the five conditions in each run. Trials recurred in a pseudo-random order, whereby each condition was presented no more than twice in a row, and in equal numbers of times in each quarter of the run. Trials were separated by 24 s to minimize sensory habituation. At the onset of each trial, a visual cue ('Sniff now') prompted subjects to make a 2 s sniff, during which time the first odourant of the stimulus pair was presented. A second 'Sniff now' cue was presented 4.25 s later to prompt the second sniff, after which subjects pressed one of two buttons to indicate whether an odour was present or absent during the second sniff.

Importantly, the use of an odour detection task, rather than a higher-order task of odour discrimination or memory, imposed few cognitive demands on the patients with Alzheimer's disease, helping

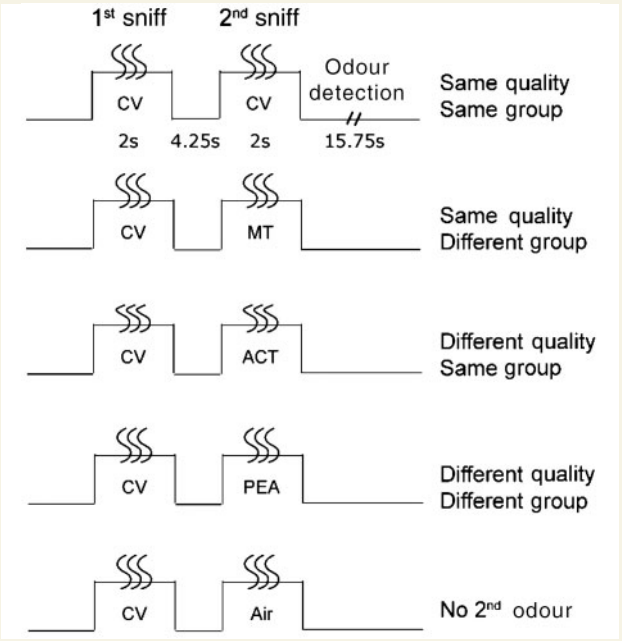

Figure 2 Experimental paradigm. Four odourant pairs systematically varying in odour quality and odourant functional group were presented in an olfactory cross-adaptation paradigm, constituting a 2×2 factorial design. A fifth pair with odourant as the first sniff and odourless air as the second sniff was presented as a filler trial. Examples of the odourant pairings that comprise the different conditions are shown here. ACT = acetophenone; CV = carvone; MT = menthol; PEA = phenethyl alcohol.

to minimize online performance confounds that could have influenced fMRI activation patterns. Along these same lines, to reduce patient reliance on working memory to perform the task, button presses on each trial were always prompted by two visual cues ('yes odour' and 'no odour', presented on left and right sides of the computer screen) to indicate which button corresponded to which response alternative. Lastly, each participant underwent a practice session before entering the scanner to ensure that the required procedures were successfully mastered.

Behavioural testing

Prior to scanning, subject-specific odour detection thresholds for phenethyl alcohol, a pure olfactant, were measured with the Sniffin' Sticks Threshold Test (Hummel *et al.*, 1997), using a seven-staircase-reversal procedure that has been shown to have high test-retest reliability (Doty *et al*., 1995). Odour identification was evaluated using the University of Pennsylvania Smell Identification Test (UPSIT; Doty *et al*., 1984), as well as three additional psychophysical tests to assess olfactory perception of the four odourants included in the study. First, subjects sniffed the odourants from glass jars and made ratings of odour affective valence, intensity and familiarity on 10-point Likert scales from 0 ('not at all') to 10 ('extremely'). Second, subjects smelled the odour stimuli again and indicated how 'minty' or 'floral' each odourant was, using separate 10-point Likert scales. Third, subjects sniffed from two jars successively (separated by 5 s) to judge the similarity between each pair of odourants (constituting a total of six pair-wise combinations of the four odourants), again using a 10-point Likert scale from 0 ('not at all similar') to 10 ('extremely similar/identical').

Respiratory monitoring

During scanning, subjects were affixed with a pair of breathing belts to monitor respirations online (Gottfried *et al.*, 2006; Li *et al.*, 2006). The output from these belts was transmitted to a piezo-resistive differential pressure sensor (0–1 psi, Honeywell), and the resulting analogue signal was amplified, digitized and recorded on a PC computer using a PowerLab 8/30 data acquisition system and accompanying software (ADInstruments Inc., Colorado Springs, CO). In subsequent analyses, the subject-specific sniff waveforms were baseline-adjusted by subtracting the mean signal in the 500 ms preceding sniff onset, and then averaged across each condition. Repeated measures ANOVAs were separately conducted on inspiratory volume, inspiratory duration and peak amplitude, including a group variable (Alzheimer's disease versus control) and four within-subjects variables (SG/SQ, SG/DQ, DG/SQ, DG/DQ).

Imaging

Gradient-echo T_2-weighted echoplanar images were acquired with blood-oxygen-level-dependent (BOLD) contrast on a Siemens Trio 3T MRI scanner, using an eight-channel head coil and an integrated parallel acquisition technique known as GeneRalized Autocalibrating Partially Parallel Acquisition (GRAPPA) to improve signal recovery in medial temporal and basal frontal regions (Li *et al.*, 2006). Imaging parameters were: repetition time = 2 s; echo time = 20 ms; slice thickness = 2 mm; gap = 1 mm; in-plane resolution = 1.72×1.72 mm; field of view = 220×220 mm, matrix size = 128 mm. Image acquisition was tilted at 30° to further reduce susceptibility artefact in olfactory areas. A total of 1000 volumes (24 interleaved slices per volume covering piriform and orbitofrontal cortices) was obtained over the two runs. High-resolution ($1 \times 1 \times 1$ mm) T_1-weighted anatomical scans were acquired between the two functional runs. Also, a whole-brain echoplanar image was obtained to aid with spatial coregistration between the functional (partial) echoplanar image and anatomical images (see below).

Functional MRI data analysis

The fMRI data were pre-processed using SPM2 (http://www.fil.ion.ucl.ac.uk/spm/). After the first five 'dummy' volumes were discarded to permit T_1 relaxation, images were spatially realigned to the first volume of the first session, coregistered to the single-subject whole-brain echoplanar image, and temporally adjusted using slice timing correction. Because cortical volume can decline with age, and particularly in patients with Alzheimer's disease, imaging data were not normalized to a standard echoplanar image template. Instead, we coregistered each subject's high-resolution T_1 image to his or her whole-brain echoplanar image and drew anatomical regions of interest based on the coregistered T_1 image. The regions of interest of piriform cortex (anterior and posterior), orbitofrontal cortex, amygdala and hippocampus were drawn using MRIcro (Rorden and Brett, 2000), with reference to a human brain atlas (Mai *et al.*, 1997). Two trained research assistants blind to the study drew the regions of interest, in order to minimize experimenter bias in defining these regions of interest.

Furthermore, since neurovascular coupling may differ between older and younger adults (Buckner *et al*., 2000; D'Esposito *et al*., 2003), we chose to convolve the condition-specific vectors of onset times with a

finite impulse response function (2 s time-bins), rather than a canonical haemodynamic response function, to model the brain activity. Five vectors, consisting of the four odourant conditions and the control condition, were timelocked to the onset of the first sniff and entered into the model as regressors. Six movement-related parameters (derived from spatial realignment) were also entered as covariates of no interest.

Beta values at each time-bin specified in the finite impulse response model were estimated using the general linear model (Friston *et al.*, 1995) in SPM2, providing a time course of brain activity for each voxel and for each condition. Inspection of these time courses revealed a distinct temporal difference between the brain responses of the two groups (Fig. 4B), such that the peaks of activity corresponding to the first and second sniff occurred one time-bin later in the Alzheimer's disease group compared with the control group. Due to this temporal difference, activity attributed to the first sniff was averaged across time-bins 2–4 for the control group and time-bins 3–5 for the Alzheimer's disease group. Activity attributed to the second sniff was averaged across time-bins 4–6 for the control group and time-bins 5–7 for the Alzheimer's disease group. A difference score was then calculated by subtracting the second sniff beta from the first sniff beta, and this score was averaged across all voxels in a given region of interest. By this calculation, a positive score denotes a reduction in beta from the first to second sniff, i.e. an fMRI adaptation effect. For display, beta values were converted to percent signal change. Two types of analyses were conducted:

(1) Region-of-interest analysis. In order to test for quality-related adaptation in a given brain region, we compared the difference scores from the same quality condition (ΔSQ, collapsed across same quality/same group and same quality/different group) to the scores from the different quality condition (ΔDQ, collapsed across different quality/same group and different quality/different group) within each group of subjects. As noted above, effects were averaged across all voxels in the region of interest. A similar analysis was performed to test for functional group-related adaptation, this time comparing the same group condition (ΔSG, collapsed across same quality/same group and different quality/same group) with the different group condition (ΔDG, collapsed across same quality/different group and different quality/different group).

(2) Voxel-level analysis. In a separate approach, we examined the spatial extent of voxels exhibiting odour quality adaptation by: (i) identifying the number of quality-responsive voxels (from the region-of-interest analysis described above) that exceeded a liberal threshold ($P<0.05$ uncorrected), individually for each subject; (ii) converting these numbers into percentages of all voxels within the anatomical region of interest (to correct for patient-specific differences in brain size); and then (iii) comparing these percentages of cross-adapting voxels between the Alzheimer's disease and control groups. Finally, in order to assess how the voxel-level analysis specifically informs the region-of-interest results, the effect size of odour quality adaptation (i.e. the 'difference' beta between ΔSQ and ΔDQ) was estimated for each voxel within a region of interest and compiled into frequency histograms, using 0.5-beta bin-increments, separately for Alzheimer's disease and control groups. These response distributions were then fit with a standard Gaussian function in Matlab to test whether the disruption of odour quality coding in Alzheimer's disease was broadly or sparsely distributed across the population of voxels.

Results

Behavioural

Subject scores on the MMSE, a general index of cognitive function (Folstein *et al.*, 1975), were significantly reduced in the Alzheimer's disease group, in keeping with the diagnosis of mild probable Alzheimer's disease in this patient cohort (Table 1). Notably, there was no significant group difference in odour detection thresholds (Sniffin' Sticks Threshold Test), suggesting that basic olfactory capabilities in patients with Alzheimer's disease and elderly controls were similarly preserved. On the other hand, odour identification, as measured by the University of Pennsylvania Smell Identification Test, was significantly lower in the Alzheimer's disease group, in comparison with the control group.

Subjects also provided perceptual ratings of the four odourants used in the imaging study. There were no significant rating differences in odour intensity, pleasantness or familiarity across the stimuli in either the Alzheimer's disease or control group (repeated-measures ANOVAs; P's >0.1), nor did these ratings significantly differ between the Alzheimer's disease and control groups (P's >0.2, Fig. 3A). On the other hand, analysis of the odour quality ratings (Fig. 3B, left two columns) indicated that the Alzheimer's disease subjects had considerable difficulty discerning the qualitative characteristics of the odourants: whereas the control group rated the minty odourants more 'minty' than 'floral' ($P=0.01$; Wilcoxon two-tailed test) and rated the floral odourants more 'floral' than 'minty' ($P=0.01$), the Alzheimer's disease group rated the 'floral' and 'minty' notes equally strongly for the minty odourants ($P=0.51$) and for the floral odourants ($P=0.30$). Examination of the odour pair-wise similarity ratings further confirmed that patients with Alzheimer's disease were preferentially impaired on higher-order olfactory discrimination. Patients with Alzheimer's disease perceived the qualitatively different (DQ) odourant pairs to be just as similar as the qualitatively similar (SQ) pairs ($P=0.11$; Fig. 3B, right column), in comparison with the control subjects who found the different quality pairs less similar than the same quality pairs ($P=0.05$). Importantly, the similarity ratings and the floral/minty ratings were significantly correlated on a subject-by-subject level, $R=0.53$, $P<0.05$, suggesting strong convergence validity of these measures tapping odour quality perception.

Table 1 Subject characteristics (means ± SD)

	Alzheimer's group ($n=10$)	Control group ($n=10$)
Age	75.7 ± 4.1	76.3 ± 3.9
Male/female	4/6	4/6
Right/left-handed	10/0	9/1
MMSE (0–30)*	25.0 ± 2.8	29.2 ± 0.9
Odour detection threshold (1–16)	6.0 ± 3.6	7.8 ± 3.0
Odour identification (0–40)*	18.1 ± 6.1	29.7 ± 3.5

*$P<0.05$.

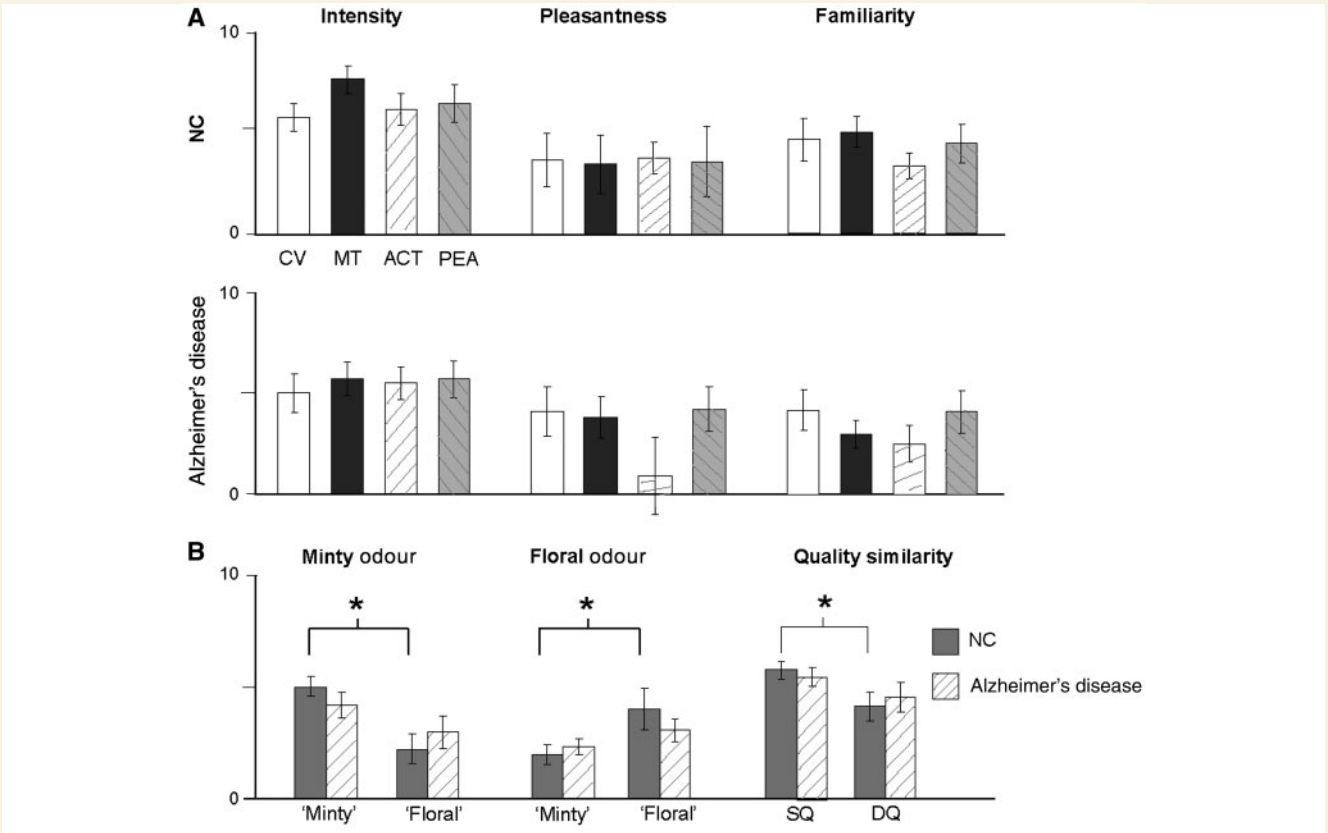

Figure 3 Olfactory psychophysical ratings. (**A**) Perceptual ratings of intensity, valence and familiarity for the four odourants, averaged across control and Alzheimer's disease groups. (**B**) Odour ratings of 'floweriness' and 'mintiness' for the floral odourants (average of ACT and PEA ratings) and for the minty odourants (average of CV and MT ratings) (left two panels), and similarity ratings of odour quality between all pair-wise combinations of odourants (right panel). $*P < 0.05$. ACT = acetophenone; CV = carvone; MT = menthol; PEA = phenethyl alcohol; NC = controls.

Region-of-interest analysis: odour quality-related cross-adaptation in PPC

Based on our hypothesis that a defect in odour quality coding should impede olfactory identification and discrimination, we asked whether neural representations of odour quality, as indexed via fMRI adaptation, are functionally disrupted in central brain areas where the neuropathological lesions of Alzheimer's disease first accumulate, over and above any non-specific effects of ageing *per se*. As noted above, to minimize performance confounds between groups, subjects were not instructed to make odour quality judgements during scanning.

In healthy elderly control subjects, presentation of qualitatively similar (versus qualitatively different) odourant pairs elicited significant cross-adapting (decreased) fMRI activity in left PPC ($T_9 = 2.24$, $P = 0.05$), in keeping with our earlier findings in healthy young subjects (Gottfried *et al.*, 2006). Time-course plots of PPC activity (Fig. 4A, left) illustrate that sequential presentation of different quality odourants was associated with a biphasic response profile (with peaks at 3 and 5 repetition times, or 6 and 10 s), suggesting that our technique has sufficient resolution to distinguish between the two sniff events. In comparison with different-quality trials, which exhibited minimal response change from first to second sniff, there was a steep decline in fMRI activation with similar-quality trials. Critically, this cross-adaptation effect in PPC was specific for odour perceptual quality, without generalization to odourant structural features. In left and right PPC, the effect of chemical functional group on fMRI adaptation was statistically similar for same-group and different-group odourant pairs (T's < 0.30, P's > 0.77), implying that there was no differential influence of odourant functional group on olfactory coding in this brain region (Fig. 4A, right), and in keeping with our prior findings (Gottfried *et al.*, 2006).

In contrast, patients with mild-stage Alzheimer's disease exhibited a very different activity pattern in PPC. Presentation of similar-quality and different-quality odourant pairs elicited comparable magnitudes of fMRI adaptation in PPC (Fig. 4B, left) that were not statistically different (left PPC, $T_9 = -0.55$, $P = 0.59$; right PPC, $T_9 = -0.86$, $P = 0.41$). Comparison with the control group response time-courses in PPC indicates that the absence of quality-specific effects in the Alzheimer's disease group reflected non-specific fMRI adaptation to the different-quality trials, rather than a lack of fMRI adaptation to the similar-quality trials (with a significant between-group interaction: $P < 0.05$, one-tailed). Interestingly, with regard to odourant functional group, the Alzheimer's disease group demonstrated an unexpected

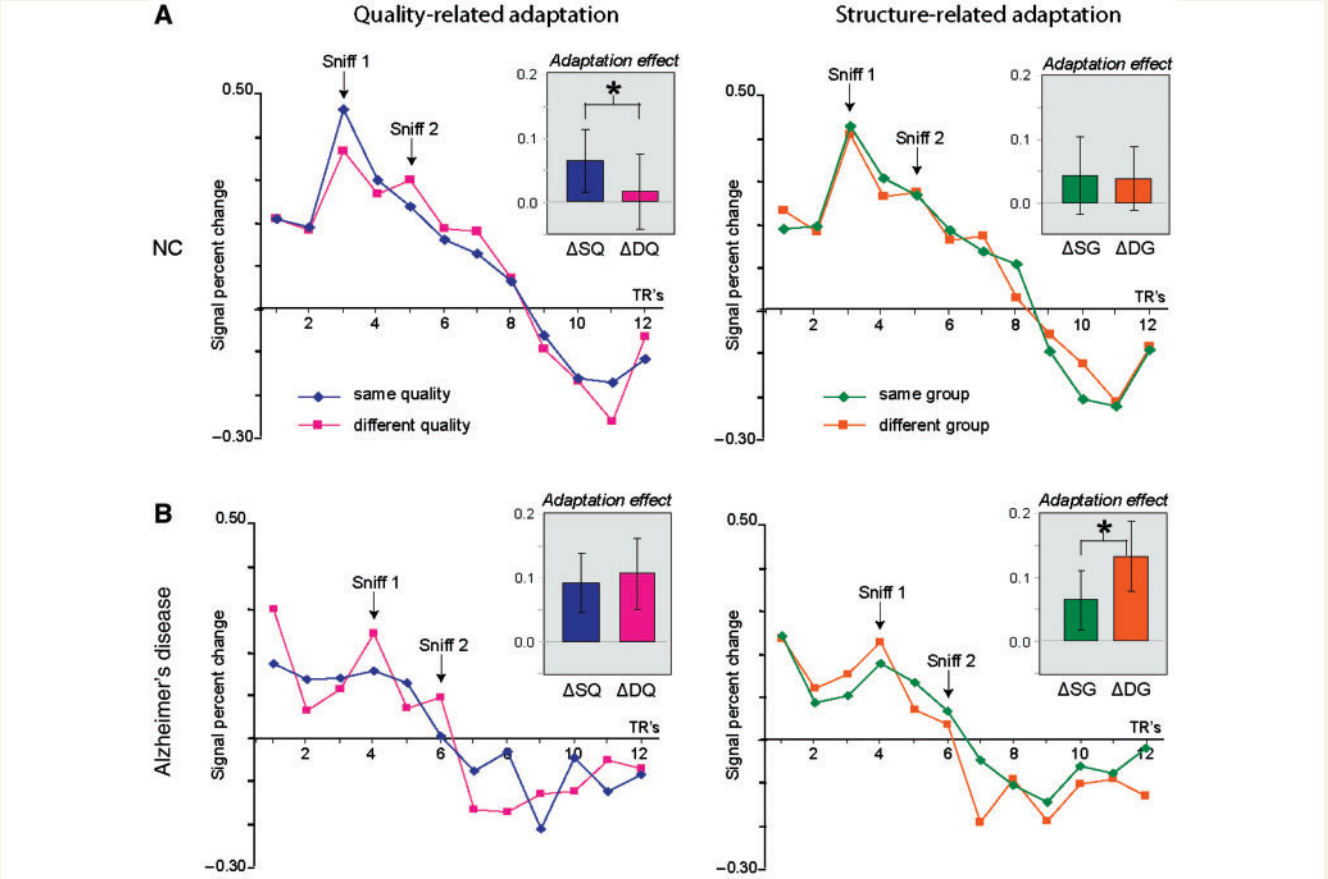

Figure 4 Cross-adaptation effects in the left posterior piriform cortex. (**A**) In normal control subjects, sequential presentation of odourants similar in quality elicited reliable fMRI adaptation upon the second sniff, when compared with odourants different in quality (left panel) ($P = 0.05$). In contrast, the magnitude of fMRI adaptation did not differ for odourants containing the same or different molecular functional group (right panel). (**B**) Patients with Alzheimer's disease failed to demonstrate selective cross-adaptation in response to either odour quality of odourant functional group. Paradoxical response facilitation was observed following presentation of a structurally unrelated odour ($P = 0.05$). Insets illustrate the effect sizes of fMRI adaptation. SQ = same quality; DQ = different quality; SG = same functional group; DG = different functional group; NC = controls; RT = repetition time (error bars, ± SEM). $^{*}P < 0.05$.

profile of 'reversed' fMRI adaptation, in which there was greater PPC response decline for the different group pair than for the same group pair (left PPC: $T_9 = -2.28$, $P = 0.05$; right PPC, at trend: $T_9 = -1.83$, $P = 0.10$) (Fig. 4B, right).

We also explored the regional specificity of these cross-adaptation effects by conducting the same analysis in other olfactory brain areas, including the anterior piriform cortex, amygdala, hippocampus and orbitofrontal cortex. Planned contrasts of differential betas failed to indicate any significant main effect of quality-specific fMRI adaptation in either the control or the Alzheimer's disease group in any of the regions (P's > 0.15). In contrast to our previous findings in young healthy subjects (Gottfried *et al.*, 2006), the absence of odour quality repetition in hippocampus or orbitofrontal cortex may imply a non-specific age effect that impacts on olfactory coding in these brain regions. Finally, anterior piriform cortex in the Alzheimer's disease group also exhibited an effect of reversed fMRI adaptation with more response reduction for the different group pair than for the same group pair (left anterior piriform cortex: $T_9 = -2.23$, $P = 0.05$; right anterior piriform cortex, at trend: $T_9 = -1.98$, $P = 0.08$).

In an effort to disentangle the effects that cognitive loss *per se* might have on the odour adaptation disruption in the Alzheimer's disease group, we also examined Alzheimer's disease subject-wise correlations between MMSE scores and the magnitude of fMRI quality-adaptation in both left and right PPC. Neither of these correlations was significant (R's < 0.32, P's > 0.38), suggesting that the breakdown of quality-related olfactory adaptation in the Alzheimer's disease group was not systematically related to their cognitive deficits.

Voxel-level analysis: extent and distribution of quality adaptation effects in PPC

The above results indicate that odour quality coding is disrupted in PPC in patients with mild Alzheimer's disease. We then set out to examine the overall spatial extent of quality-responsive voxels

remaining in left PPC, and to explore how this was related to the magnitude of fMRI cross-adaptation, on a patient-by-patient basis. For each subject, we calculated the proportion of voxels in left PPC that exhibited adaptive fMRI responses to qualitatively similar (versus different) odour pairs, at a liberal threshold of $P<0.05$ (uncorrected). The mean percentage of quality-adapting voxels in patients with Alzheimer's disease was $1.9\pm1.6\%$ (mean $\pm$ SD), significantly lower than that of control subjects ($5.5\pm3.9\%$) ($T_{18}=2.75$, $P=0.01$). Critically, the extent of quality-adaptive PPC voxels was strongly correlated across subjects with the overall quality adaptation effect size in left PPC ($R=0.66$, $P=0.001$) (Fig. 5). Of note, this association was independent of general olfactory responsivity in PPC: the percentage of odour-responsive voxels (identified in the contrast of all first odour-evoked activity versus baseline, $P<0.05$ uncorrected) was not correlated with the magnitude of adaptation ($R=0.17$, $P>0.48$).

To gain a better understanding of the relationship between the regional magnitude (cf. Fig. 4B) and the voxel-level extent (cf. Fig. 5) of fMRI cross-adaptation in PPC, we computed group-specific histograms reflecting frequency distributions of the cross-adaptation effect across all PPC voxels (Fig. 6). We reasoned that two different kinds of voxel-level abnormalities could account for the region of interest-level findings in Alzheimer's disease, each of which would yield a different histogram profile in comparison with the control group. If the region-of-interest effect in PPC was due to a reduced adaptation effect across the whole population of piriform voxels, then the Alzheimer's disease histogram would reveal a 'left shift' in the entire voxel frequency distribution (red line), compared with the control group (grey line) (Fig. 6A). Distributions in both groups would conform to a Gaussian function, though in Alzheimer's disease, the peak (mean) would occur at a smaller effect size (left-shifted) along the *x*-axis. On the other hand, if the region-of-interest effect were due to a reduced adaptation effect across just a subset of voxels, specifically those quality-adapting voxels at the right tail of the curve, the Alzheimer's disease histogram will approximate a left-skewed non-Gaussian distribution (Fig. 6B). Accordingly, this scenario would be driven by a reduction of coding specificity in a subset of voxels, which still might blunt the mean activity in the PPC region of interest despite functional preservation of quality coding in the majority of PPC voxels.

The data are consistent with the first hypothesis proposed above: histograms of voxel-level fMRI adaptation suggest that the adaptation effect was evenly distributed across left PPC for both Alzheimer's disease and control groups, each closely conforming to a Gaussian function (Alzheimer's disease: $R^2=0.98$; control: $R^2=0.97$), but with the mean of the distribution left-shifted for Alzheimer's disease compared with controls (compare red and grey vertical lines; Fig. 6C). In a complementary analysis, the strength of Gaussian curve fitting (R value) was calculated separately for each subject, and then the set of fits for the patients with Alzheimer's disease was compared with the set of fits for the control subjects. Mean R's (SDs) computed in this manner did not statistically differ for Alzheimer's disease and control groups: 0.97 (0.03) and 0.98 (0.02), respectively ($Z=0.49$, $P=0.62$; Wilcoxon rank-sum test). Therefore, based on these findings, the derangement of odour quality coding in Alzheimer's disease appears to be fairly widespread throughout the population of voxels in PPC, rather than being restricted to a sparse or highly focal subset of PPC voxels.

Respiratory

Online measures of respiration were obtained during scanning for each participant, enabling us to assess whether there were group-specific differences in sniffing and, of equal importance, to ensure that the patients with Alzheimer's disease successfully maintained the two-sniff task throughout the course of the experiment. Sniffing parameters, including inspiratory volume, inspiratory duration and peak amplitude, did not significantly differ

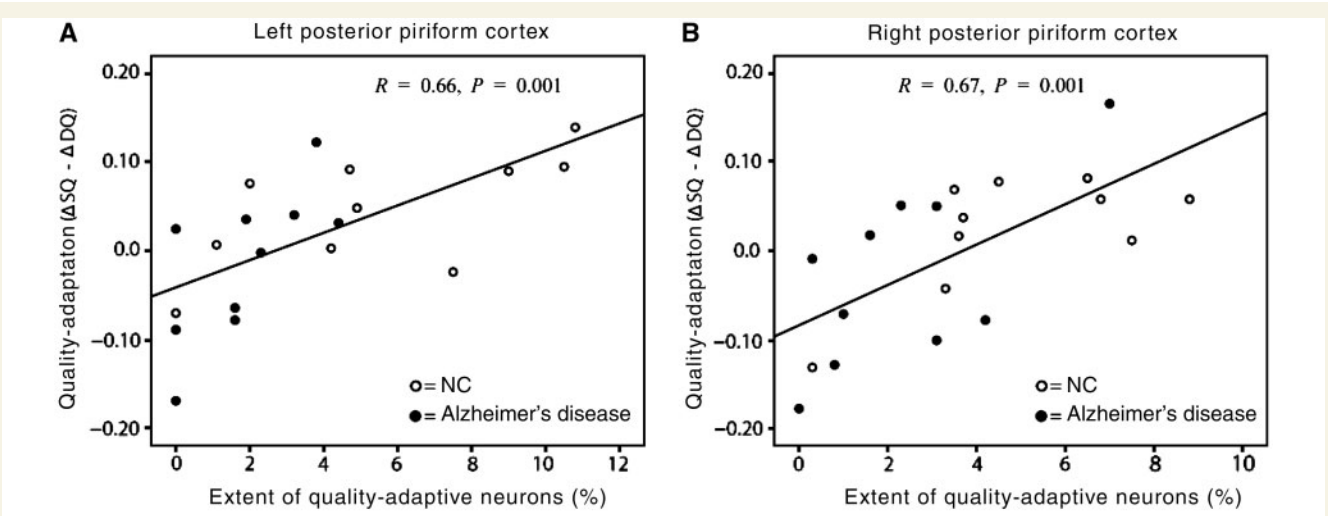

Figure 5 Subject-wise correlation analysis regressing the magnitude of quality-specific cross-adaptation against the spatial extent of quality-adaptive voxels, separately within left and right PPC, across the control group (open circles) and the Alzheimer's disease (closed circles) group. Each dot represents data from a different subject.

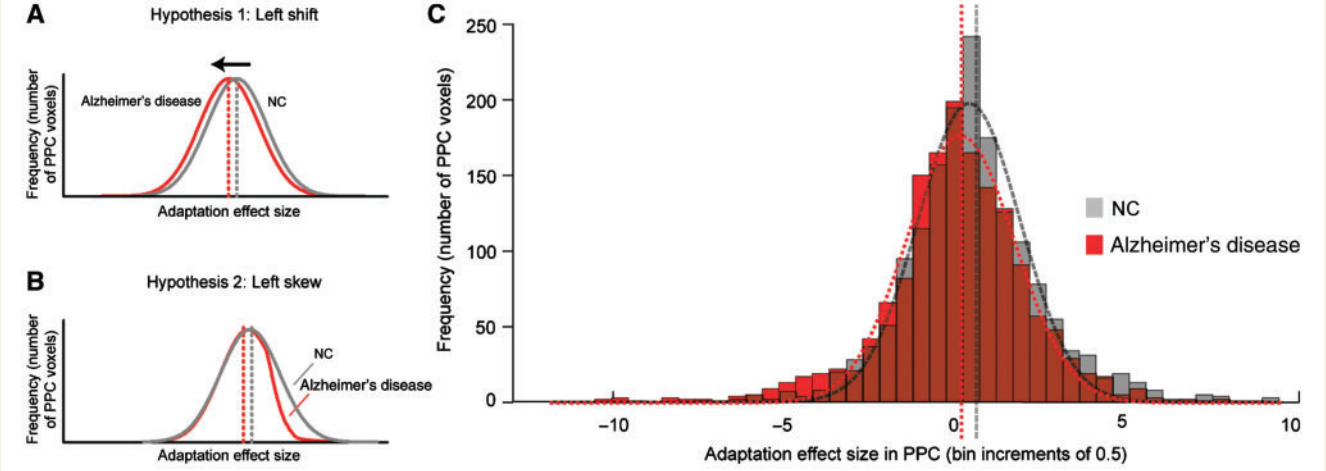

Figure 6 Histograms depicting the frequency distributions (in numbers of voxels) for different effect sizes of odour quality adaptation in left PPC. (**A**) A hypothetical profile shows that the voxel distribution is left-shifted for Alzheimer's disease compared with control (NC). (**B**) An alternative hypothetical profile shows that the voxel distribution is left-skewed for Alzheimer's disease compared with control. (**C**) Histogram plots of voxel-level data (voxels pooled from all subjects in each group) indicate that the distribution of the Alzheimer's disease group (red) is shifted to the left, in comparison with the control group (grey), consistent with hypothesis (**A**) above. Histogram areas containing overlapping information between the two groups are shown in brown. Dashed curves represent Gaussian fits to each distribution. Vertical lines mark the mean fMRI magnitudes of odour quality adaptation determined from the region-of-interest analyses depicted in Fig. 4.

across odour conditions ($P = 0.65$), between patients with Alzheimer's disease and control subjects ($P = 0.58$), or interactively between odour condition and group ($P = 0.74$) (Fig. 7). That both groups made timely and comparable first and second sniffs following the 'Sniff now' command demonstrated satisfactory compliance with the instructions and confirmed that the patients with Alzheimer's disease received odour stimulation as designed.

Discussion

By combining psychophysical measures of odour identification with an fMRI cross-adaptation paradigm, we established that in patients with mild-stage Alzheimer's disease, perceptual impairment of odour quality discrimination occurs in conjunction with a disruption of odour quality coding in PPC (Fig. 4). These effects were observed despite matched odour detection thresholds for Alzheimer's disease and control groups. In addition, the percentage of PPC voxels exhibiting quality-adaptive responses showed a decline in patients with Alzheimer's disease, compared with age-matched controls, accounting for 44% of the total variance (R^2) in the overall magnitude of fMRI cross-adaptation (Fig. 5). That the disruption of fMRI adaptation appears evenly distributed over the population of PPC voxels in Alzheimer's disease suggests a general disorganization of odour quality coding in this region (as opposed to a patchy or sparse effect) as a result of Alzheimer's disease neuropathology. These translational research findings follow closely from predictions based on our previous work (Gottfried *et al.*, 2006) about how odour quality information is encoded in the healthy human brain, and they provide one of the first mechanistic accounts for the well-recognized olfactory perceptual deficits in early Alzheimer's disease.

Insofar as cognitive decline in the patients with Alzheimer's disease could have independently contributed to the group differences in fMRI adaptation, it is important to emphasize that our study was explicitly designed to minimize such a confound. In particular, the use of a low-level odour detection task (rather than an odour discrimination task) during scanning helped eliminate the chance that greater cognitive effort in the Alzheimer's disease group could have biased the results. In other words, neither patients with Alzheimer's disease nor control subjects were asked to perform a discrimination task while in the scanner, precisely to ensure that perceptual differences in odour discrimination performance could not have confounded the results. The fact that Alzheimer's disease and control groups were matched for odour detection thresholds (Table 1) and complied equally well with the two-sniff task instruction (Fig. 7) further demonstrates that the two groups were matched in olfactory performance and demand during the fMRI experiment, excluding the confound of cognitive disparity between the two samples. Finally, the lack of a significant subject-wise correlation between Alzheimer's disease cognitive status (MMSE score) and magnitude of fMRI adaptation in PPC additionally suggests that cognitive deficits *per se* had no direct bearing on the imaging results in Alzheimer's disease.

It thus seems likely that the observed disorganization of PPC cross-adaptation in patients with Alzheimer's disease is due to defective odour quality coding in PPC. This is not to say that the defect of odour quality coding in PPC is necessarily selective for Alzheimer's disease. Indeed, other neurodegenerative disorders with olfactory perceptual deficits, including Parkinson's disease and Huntington's disease (Nordin *et al.*, 1995; Mesholam *et al.*, 1998), are likely to target olfactory-related limbic areas, and it follows that similar defects of fMRI odour quality adaptation might be seen in these conditions. These observations underscore

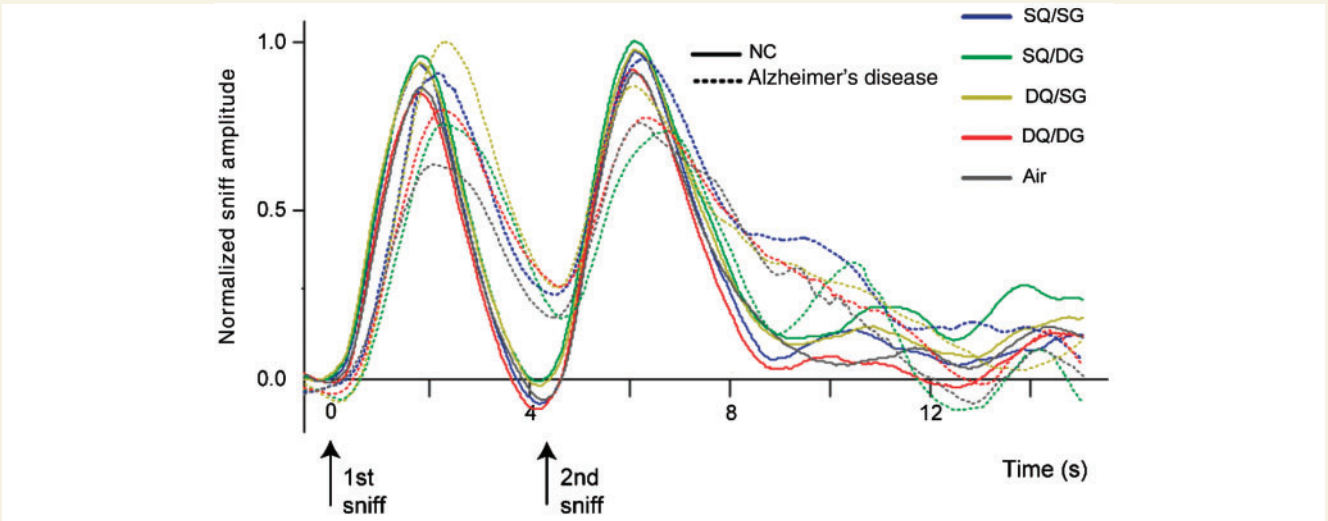

Figure 7 Plots illustrate the two-sniff respiratory profiles for control (NC) and Alzheimer's disease groups, averaged across each condition. Waveforms were time-locked to the onset of the first sniff and normalized to the maximal amplitude within each subject.

the principal goal of our study to elucidate the mechanisms underlying olfactory perceptual dysfunction in Alzheimer's disease—the neural basis of which has been largely unexplored—rather than to establish the specificity of these mechanisms to Alzheimer's disease. The application of a hypothesis-driven framework, drawing from our findings in healthy subjects (Gottfried *et al.*, 2006), has provided a novel way of exploring the neuroscientific aspects of olfactory perceptual impairment in Alzheimer's disease.

It is also worth noting that the effects reported here are not necessarily specific to the piriform region. For example, in the absence of concurrent measurements of activity in the olfactory bulb and anterior olfactory nucleus, it remains possible that a pathological deficit upstream to PPC could partially account for the observed findings. However, the robustness of 'first-sniff' odour-evoked responses in PPC (statistically comparable magnitudes in Alzheimer's disease and control groups, $P = 0.20$), the perceptual specificity of the effects and the preservation of odour detection thresholds (in comparison with the control group) together suggest that the flow of olfactory information from the periphery to piriform cortex is largely uninterrupted in the patients with Alzheimer's disease.

Interestingly, the absence of quality-specific cross-adaptation in Alzheimer's disease stemmed from comparable posterior piriform response suppression to odours of similar and different qualities, rather than a lack of suppression to the similar odour pairs. This generalized 'adaptation' effect coincides well with our schematic model of odour quality miscoding in Alzheimer's disease (Fig. 1B), which hypothesizes that a widening of population tuning curves in PPC leads to progressive loss of coding specificity. As a consequence, fMRI adaptation in PPC would be expected to occur just as likely for odour qualities outside the tuning range as it would for odour qualities optimally within the tuning range. In principle, these results may additionally reflect a generalized response fatigue, whereby PPC is unable to sustain excitability during repeated olfactory stimulation in spite of distinct odour qualities. This complementary mechanism accentuates the idea that pathological changes in PPC disrupt odour-specific firing profiles, to the extent that responses to new smells cannot be preserved. Such a framework would be consistent with the psychophysical data showing that patients with Alzheimer's disease were essentially unable to extract quality-specific information from the different odourants during identification and discrimination tasks.

The concomitant dysfunction of odour quality processing at both the behavioural and neural levels in Alzheimer's disease holds important implications for clarifying the functional organization of the human olfactory system. As discussed earlier, converging evidence in the literature suggests that odour quality coding in humans is subserved by PPC (Gottfried *et al.*, 2006; Li *et al.*, 2006, 2008; Howard *et al.*, 2009), but these data are restricted to neuroimaging studies in healthy subjects, from which one can infer correlation but not causation. Here, the regional disruption of odour-adaptive responses in PPC—specifically in an area of medial temporal lobe overlapping with the initial site of Alzheimer's disease neuropathology—highlights the key involvement of PPC in the perceptual coding of odour quality. Thus, to the extent that the current study can be considered a lesion model of olfactory limbic brain function, it is plausible to infer causal evidence for PPC being a necessary substrate of odour object recognition.

An unexpected finding was the reversal of the fMRI cross-adaptation effect for odourant molecular functional group in the PPC of patients with Alzheimer's disease. Specifically, the first-sniff presentation of a given odourant actually induced greater habituation in voxels responsive to different functional groups, such that second-sniff presentation of same group evoked greater activity than that of different group. This result presumably reflects abnormal structure coding as a result of Alzheimer's disease neuropathology, though it is important to note that PPC has no apparent role in functional group coding in healthy young individuals (Gottfried *et al.*, 2006), suggesting that this region has become

more stimulus driven in Alzheimer's disease. For example, one possibility is that repetition of the same odourant functional group effectively comprises twice the stimulus input, eliciting a relative summation of odour-evoked responses, or a suprathreshold level of activation, at the time of the second sniff, compared with single presentations of different group odourants whose inputs do not summate. Alternatively, this 'gain-of-dysfunction' response profile in Alzheimer's disease may underscore a derangement, or compensation, of information exchange between PPC and orbitofrontal cortex, or between PPC and anterior piriform cortex, all of which are reciprocally connected, or even a region-by-condition haemodynamic disruption in neurovascular coupling (Buckner *et al*., 2000; D'Esposito *et al*., 2003). These different possibilities are not mutually exclusive; at any rate, this paradoxical finding awaits future investigation.

While our study does not address underlying pathophysiological mechanisms, it is likely that the disruption of odour coding in PPC arises from a variety of effects. For example, the early accumulation of Alzheimer's disease cytopathology in the medial temporal lobe, including piriform cortex, can induce direct neuronal and synaptic loss (Yankner *et al*., 2008; Arendt, 2009; Giannakopoulos *et al*., 2009). Such a process would be in keeping with the current data indicating that the proportion of PPC voxels preferentially adapting to similar versus different odour qualities is diminished in the Alzheimer's disease group. Neurodegenerative changes can also impact on neuronal function irrespective of neuronal loss. Alzheimer's disease-related decreases in dendritic spine density, synaptic failure and impaired synaptic plasticity (Yankner *et al*., 2008; Arendt, 2009; Giannakopoulos *et al*., 2009) would cause a disorganization—or a failure to maintain the organization—of odour quality information across piriform cortical ensembles. Alternatively, to the extent that piriform codes of odour quality rely on feedback from olfactory-related brain regions such as orbitofrontal cortex or entorhinal cortex, a pathological disruption in these circuits could indirectly impair coding specificity in PPC. In addition, on the basis of animal models suggesting that acetylcholine can enhance olfactory perceptual learning, reduce interference among stored odour memories and support fine odour discrimination in piriform cortex (Hasselmo *et al*., 1992; Saar *et al*., 2001; Wilson, 2001), our results would be consistent with the profound perturbation of cholinergic innervation to the medial temporal lobes that is a hallmark of Alzheimer's disease (Geula and Mesulam, 1996; Mesulam, 2004).

We note that some of the reported null effects might have arisen from insufficient statistical power due to the use of a relatively small study sample (10 participants each in the Alzheimer's disease and control groups). This limitation is especially pertinent to measurement of odour detection thresholds (Table 1), testing of which can be highly variable and correlated to odour identification performance (Doty *et al*., 1994). It thus remains possible that an impairment of odour sensitivity is already present in early stages of Alzheimer's disease, but because of a lack of power, any such threshold differences between Alzheimer's disease and control groups would have been missed in the present study. Future research with a larger cohort of patients with Alzheimer's disease may help to elucidate this issue, thereby further disambiguating basic and higher-level mechanisms that contribute to the neural disruption of olfactory processing.

In summary, the imaging results presented here demonstrate that odour quality coding is disorganized in limbic olfactory regions that are early targets of Alzheimer's disease pathology. That two separate fMRI measures of odour quality (adaptation magnitude and spatial extent) were both diminished in the Alzheimer's disease group attests to the robustness of the technique and helps validate the use of fMRI cross-adaptation as a sensitive probe of limbic olfactory function. With the emergence of novel therapeutic and preventative interventions for Alzheimer's disease on the horizon (Sigurdsson, 2009), the need for novel diagnostic tools, particularly for asymptomatic stages, and before irreversible neuropathological damage sets in, will become increasingly imperative. The current study warrants future longitudinal investigations among high-risk groups (e.g. individuals with mild cognitive impairment, or ApoE4) (Bacon *et al*., 1998; Larsson *et al*., 1999; Calhoun-Haney and Murphy, 2005; Wilson *et al*., 2007) to assess the prevalence of defective odour quality coding in these populations and to explore the predictive validity of fMRI odour quality adaptation as an adjunctive diagnostic biomarker that can distinguish healthy elderly individuals with age-associated smell loss (Murphy *et al*., 2002) from those on a clinical trajectory towards Alzheimer's disease.

Acknowledgements

The authors thank Kryzstof Bujarski for conducting neurological diagnostic interviews and olfactory assessments to pre-select research participants, and Katie Phillips and Leonardo Lopez for assistance in data collection and analysis. The authors are also thankful to Nancy Johnson, Sandra Weintraub and the research coordinators of the Northwestern Alzheimer's Disease Centre for assistance with patient recruitment, and to Marsel Mesulam for helpful advice and discussions.

Funding

This research was supported by grants to J.A.G. from the Northwestern Alzheimer's Disease Centre/National Institute on Aging, the Alzheimer's Disease Research Fund at the Illinois Department of Public Health, and the National Institute for Deafness and Other Communication Disorders.

References

Arendt T. Synaptic degeneration in Alzheimer's disease. Acta Neuropathol 2009; 118: 167–79.

Averback P. Two new lesions in Alzheimer's disease. Lancet 1983; 2: 1203.

Bacon AW, Bondi MW, Salmon DP, Murphy C. Very early changes in olfactory functioning due to Alzheimer's disease and the role of apolipoprotein E in olfaction. Ann NY Acad Sci USA 1998; 855: 723–31.

Braak H, Braak E. Neuropathological stageing of Alzheimer-related changes. Acta Neuropathol 1991; 82: 239–59.

Buchsbaum MS, Kesslak JP, Lynch G, Chui H, Wu J, Sicotte N, et al. Temporal and hippocampal metabolic rate during an olfactory memory task assessed by positron emission tomography in patients with dementia of the Alzheimer type and controls. Preliminary studies. Arch Gen Psychiatry 1991; 48: 840–7.

Buckner RL, Goodman J, Burock M, Rotte M, Koutstaal W, Schacter D, et al. Functional-anatomic correlates of object priming in humans revealed by rapid presentation event-related fMRI. Neuron 1998; 20: 285–96.

Buckner RL, Snyder AZ, Sanders AL, Raichle ME, Morris JC. Functional brain imaging of young, nondemented, and demented older adults. J Cogn Neurosci 2000; 12 (Suppl 2): 24–34.

Calhoun-Haney R, Murphy C. Apolipoprotein epsilon4 is associated with more rapid decline in odour identification than in odour threshold or Dementia Rating Scale scores. Brain Cogn 2005; 58: 178–82.

D'Esposito M, Deouell LY, Gazzaley A. Alterations in the BOLD fMRI signal with ageing and disease: a challenge for neuroimaging. Nat Rev Neurosci 2003; 4: 863–72.

Devanand DP, Liu X, Tabert MH, Pradhaban G, Cuasay K, Bell K, et al. Combining early markers strongly predicts conversion from mild cognitive impairment to Alzheimer's disease. Biol Psychiatry 2008; 64: 871–9.

Devanand DP, Michaels-Marston KS, Liu X, Pelton GH, Padilla M, Marder K, et al. Olfactory deficits in patients with mild cognitive impairment predict Alzheimer's disease at follow-up. Am J Psychiatry 2000; 157: 1399–405.

Djordjevic J, Jones-Gotman M, De Sousa K, Chertkow H. Olfaction in patients with mild cognitive impairment and Alzheimer's disease. Neurobiol Aging 2008; 29: 693–706.

Doty RL, McKeown DA, Lee WW, Shaman P. A study of the test-retest reliability of ten olfactory tests. Chem Senses 1995; 20: 645–56.

Doty RL, Reyes PF, Gregor T. Presence of both odour identification and detection deficits in Alzheimer's disease. Brain Res Bull 1987; 18: 597–600.

Doty RL, Shaman P, Kimmelman CP, Dann MS. University of Pennsylvania Smell Identification Test: a rapid quantitative olfactory function test for the clinic. Laryngoscope 1984; 94: 176–8.

Doty RL, Smith R, McKeown DA, Raj J. Tests of human olfactory function: principal components analysis suggests that most measure a common source of variance. Percept Psychophys 1994; 56: 701–7.

Folstein MF, Folstein SE, McHugh PR. "Mini-mental state", a practical method for grading the cognitive state of patients for the clinician. J Psychiatry Res 1975; 12: 189–98.

Friston KJ, Frith CD, Turner R, Frackowiak RS. Characterizing evoked hemodynamics with fMRI. Neuroimage 1995; 2: 157–65.

Geula C, Mesulam MM. Systematic regional variations in the loss of cortical cholinergic fibers in Alzheimer's disease. Cereb Cortex 1996; 6: 165–77.

Giannakopoulos P, Kovari E, Gold G, von Gunten A, Hof PR, Bouras C. Pathological substrates of cognitive decline in Alzheimer's disease. Front Neurol Neurosci 2009; 24: 20–9.

Gottfried JA, Winston JS, Dolan RJ. Dissociable codes of odour quality and odourant structure in human piriform cortex. Neuron 2006; 49: 467–79.

Grill-Spector K, Henson R, Martin A. Repetition and the brain: neural models of stimulus-specific effects. Trends Cogn Sci 2006; 10: 14–23.

Hasselmo ME, Anderson BP, Bower JM. Cholinergic modulation of cortical associative memory function. J Neurophysiol 1992; 67: 1230–46.

Hebert LE, Scherr PA, Bienias JL, Bennett DA, Evans DA. Alzheimer disease in the US population: prevalence estimates using the 2000 census. Arch Neurol 2003; 60: 1119–22.

Herzog AG, Kemper TL. Amygdaloid changes in aging and dementia. Arch Neurol 1980; 37: 625–9.

Howard JD, Plailly J, Grueschow M, Haynes JD, Gottfried JA. Odour quality coding and categorization in human posterior piriform cortex. Nat Neurosci 2009; 12: 932–8.

Hummel T, Sekinger B, Wolf SR, Pauli E, Kobal G. 'Sniffin' sticks': olfactory performance assessed by the combined testing of odour identification, odour discrimination and olfactory threshold. Chem Senses 1997; 22: 39–52.

Hyman BT, Van Hoesen GW, Damasio AR, Barnes CL. Alzheimer's disease: cell-specific pathology isolates the hippocampal formation. Science 1984; 225: 1168–70.

Kadohisa M, Wilson DA. Separate encoding of identity and similarity of complex familiar odours in piriform cortex. Proceedings of the National Academy of Sciences of the United States of America 2006; 103: 15206–11.

Kareken DA, Doty RL, Moberg PJ, Mosnik D, Chen SH, Farlow MR, et al. Olfactory-evoked regional cerebral blood flow in Alzheimer's disease. Neuropsychology 2001; 15: 18–29.

Kesslak JP, Nalcioglu O, Cotman CW. Quantification of magnetic resonance scans for hippocampal and parahippocampal atrophy in Alzheimer's disease. Neurology 1991; 41: 51–4.

Koss E, Weiffenbach JM, Haxby JV, Friedland RP. Olfactory detection and identification performance are dissociated in early Alzheimer's disease. Neurology 1988; 38: 1228–32.

Kourtzi Z, Kanwisher N. Representation of perceived object shape by the human lateral occipital complex. Science 2001; 293: 1506–9.

Larsson M, Semb H, Winblad B, Amberla K, Wahlund LO, Backman L. Odour identification in normal aging and early Alzheimer's disease: effects of retrieval support. Neuropsychology 1999; 13: 47–53.

Li W, Howard JD, Parrish TB, Gottfried JA. Aversive learning enhances perceptual and cortical discrimination of indiscriminable odour cues. Science 2008; 319: 1842–5.

Li W, Luxenberg E, Parrish T, Gottfried JA. Learning to smell the roses: experience-dependent neural plasticity in human piriform and orbitofrontal cortices. Neuron 2006; 52: 1097–108.

Mai JK, Assheuer J, Paxinos G. Atlas of the human brain. New York: Thieme; 1997.

McKhann G, Drachman D, Folstein MF, Katzman R, Price DA, Stadlan EM. Clinical diagnosis of Alzheimer's disease: report of the NINCDS-ADRDA Work Group under the auspices of Department of Health and Human Services Task Force on Alzheimer's disease. Neurology 1984; 34: 939–44.

Mesholam RI, Moberg PJ, Mahr RN, Doty RL. Olfaction in neurodegenerative disease: a meta-analysis of olfactory functioning in Alzheimer's and Parkinson's diseases. Arch Neurol 1998; 55: 84–90.

Mesulam M. The cholinergic lesion of Alzheimer's disease: pivotal factor or side show? Learn Mem 2004; 11: 43–9.

Mesulam MM. Aging, Alzheimer's Disease, and Dementia: Clinical and Neurobiological Perspectives. Oxford: Oxford University; 2000.

Moberg PJ, Doty RL, Mahr RN, Mesholam RI, Arnold SE, Turetsky BI, et al. Olfactory identification in elderly schizophrenia and Alzheimer's disease. Neurobiol Aging 1997; 18: 163–7.

Morgan CD, Nordin S, Murphy C. Odour identification as an early marker for Alzheimer's disease: impact of lexical functioning and detection sensitivity. J Clin Exp Neuropsychol 1995; 17: 793–803.

Murphy C, Cerf-Ducastel B, Calhoun-Haney R, Gilbert PE, Ferdon S. ERP, fMRI and functional connectivity studies of brain response to odour in normal aging and Alzheimer's disease. Chem Senses 2005; 30 (Suppl 1): i170–1.

Murphy C, Gilmore MM, Seery CS, Salmon DP, Lasker BR. Olfactory thresholds are associated with degree of dementia in Alzheimer's disease. Neurobiol Aging 1990; 11: 465–9.

Murphy C, Jernigan TL, Fennema-Notestine C. Left hippocampal volume loss in Alzheimer's disease is reflected in performance on odour identification: a structural MRI study. J Int Neuropsychol Soc 2003; 9: 459–71.

Murphy C, Schubert CR, Cruickshanks KJ, Klein BE, Klein R, Nondahl DM. Prevalence of olfactory impairment in older adults. JAMA 2002; 288: 2307–12.

Nordin S, Paulsen JS, Murphy C. Sensory- and memory-mediated olfactory dysfunction in Huntington's disease. J Int Neuropsychol Soc 1995; 1: 281–90.

Ohm TG, Braak H. Olfactory bulb changes in Alzheimer's disease. Acta Neuropathol 1987; 73: 365–9.

Pearson RC, Esiri MM, Hiorns RW, Wilcock GK, Powell TP. Anatomical correlates of the distribution of the pathological changes in the neocortex in Alzheimer disease. Proc Natl Acad Sci USA 1985; 82: 4531–4.

Reyes PF, Golden GT, Fagel PL, Fariello RG, Katz L, Carner E. The prepiriform cortex in dementia of the Alzheimer type. Arch Neurol 1987; 44: 644–5.

Rorden C, Brett M. Stereotaxic display of brain lesions. Behavioural Neurology 2000; 12: 191–200.

Royet JP, Croisile B, Williamson-Vasta R, Hibert O, Serclerat D, Guerin J. Rating of different olfactory judgements in Alzheimer's disease. Chem Senses 2001; 26: 409–17.

Saar D, Grossman Y, Barkai E. Long-lasting cholinergic modulation underlies rule learning in rats. J Neurosci 2001; 21: 1385–92.

Schubert CR, Carmichael LL, Murphy C, Klein BE, Klein R, Cruickshanks KJ. Olfaction and the 5-year incidence of cognitive impairment in an epidemiological study of older adults. J Am Geriatr Soc 2008; 56: 1517–21.

Sigurdsson EM. Tau-Focused immunotherapy for Alzheimer's disease and related tauopathies. Curr Alzheimer Res 2009; 6: 446–50.

Talamo BR, Rudel R, Kosik KS, Lee VM, Neff S, Adelman L, et al. Pathological changes in olfactory neurons in patients with Alzheimer's disease. Nature 1989; 337: 736–9.

Thomann PA, Kaiser E, Schonknecht P, Pantel J, Essig M, Schroder J. Association of total tau and phosphorylated tau 181 protein levels in cerebrospinal fluid with cerebral atrophy in mild cognitive impairment and Alzheimer disease. J Psychiatry Neurosci 2009; 34: 136–42.

Wilson DA. Scopolamine enhances generalization between odour representations in rat olfactory cortex. Learn Mem 2001; 8: 279–85.

Wilson RS, Schneider JA, Arnold SE, Tang Y, Boyle PA, Bennett DA. Olfactory identification and incidence of mild cognitive impairment in older age. Arch Gen Psychiatry 2007; 64: 802–8.

Yankner BA, Lu T, Loerch P. The aging brain. Annu Rev Pathol 2008; 3: 41–66.